AGU ADVANCING EARTH AND SPACE SCIENCE

Earth's Future

Correspondence to:
T. Ezer,
tezer@odu.edu

A Demonstration of a Simple Methodology of Flood Prediction for a Coastal City Under Threat of Sea Level Rise: The Case of Norfolk, VA, USA

Tal Ezer[1] (iD)

[1]Center for Coastal Physical Oceanography, Old Dominion University, Norfolk, VA, USA

Abstract Many coastal cities around the world are at risk of increased flooding due to sea level rise (SLR), so here a simple flood prediction method is demonstrated for one city at risk, Norfolk, VA, on the U.S. East Coast. The probability of future flooding is estimated by extending observed hourly water level for 1927–2021 into hourly estimates until 2100. Unlike most other flood prediction methods, the approach here does not use any predetermined probability distribution function of extreme events, and instead a random sampling of past data represents tides and storm surges. The probability of flooding for 3 different flood levels and 3 different SLR projections are calculated, and the results are consistent with more sophisticated methods. Under intermediate-low SLR projection an empirical formula is found to estimate the lower bound of flooding time, showing that water level that exceeds the high tide (Mean Higher High Water, MHHW) occurred ∼0.3% of the time in the 1960s, increased to ∼6% in 2021, and projected to occur 100% of the time by ∼2080. Under intermediate SLR projection, 1000 simulations of the probability of maximum annual water level were conducted, showing that storm surges may reach ∼2 m over MHHW by 2050 and ∼3 m over MHHW by 2100; in comparison, storm surges in Norfolk over the past 90 years reached 1.6 m only once. The method derived here could be adopted to other locations and help planning mitigations and adaptation strategies for cities at risk.

Plain Language Summary Like many coastal cities around the world, Norfolk, VA, on the U.S. East Coast is experiencing accelerated flooding. Therefore, this study estimates the probability of future flooding in the city using a simple method that combines sea level rise projections with the impacts of tides and storm surges. An empirical relation is found to estimate the percentage of time the city is flooded for any flood level and any year from 1960 to 2100. The results show for example, that major floods that occurred very rarely in the past 90 years may occur almost daily to weekly by 2100, and the largest storm surges that in the past rarely reached 1.5 m over the high tide may reach up to 3 m in the future. The method derived here could be adopted to other locations and help planning mitigations and adaptation strategies for cities at risk.

1. Introduction

Acceleration in the frequency and severity of coastal flooding is seen around the world (Buchanan et al., 2017; Cazenave & Le Cozannet, 2014; Nicholls & Cazenave, 2010; Taherkhani et al., 2020), and this is especially apparent along the U.S. East Coast, from south Florida to Boston (Alarcon et al., 2022; Boon, 2012; Domingues et al., 2018; Ezer & Atkinson, 2014; Kruel, 2016; Sweet & Park, 2014; Sweet et al., 2014, 2018, 2022; Valle-Levinson et al., 2017; Wdowinski et al., 2016). This trend, if continues, can pose increased risk for people, infrastructure and economic hardship that will require planning for future mitigations and adaptation strategies and involvement of different stakeholders (John & Yusuf, 2019; Yusuf et al., 2018), as well as mitigation against further erosion of coastlines (Mitchell & Bilkovic, 2019). While global sea level rise (SLR) and its impacts on the coast is well documented (Cazenave & Le Cozannet, 2014; Jevrejeva et al., 2009; Kopp et al., 2014), many coasts are at higher risks than others. Along the U.S. East Coast for example, the rate of local SLR is higher than global rates due to regional land subsidence (Bekaert et al., 2017; Boon et al., 2010; Buzzanga et al., 2020; Eggleston & Pope, 2013), and potential contribution from slowdown of the Atlantic Meridional Overturning Circulation (AMOC) and the Gulf Stream (GS) (Ezer, 2015; Ezer & Corlett, 2012; Ezer et al., 2013; Park & Sweet, 2015; Sallenger et al., 2012).

The U.S. East Coast and the Gulf coast are also subject to tropical storms and hurricanes. The damage of flooding during storm surges increases over time due to SLR (Buchanan et al., 2017), increase intensity of hurricanes

(Emanuel, 2011; Knutson et al., 2019), and potential increase in extreme wind waves (Lobeto et al., 2021). Recent studies demonstrate that the contribution of wind wave extremes, such as during hurricanes, is often underestimated in coastal SLR calculations (Melet et al., 2018); waves set up and swash may be especially significant for example, on sandy beaches along the U.S. West Coast (Serafin et al., 2017). Models also show that under high-emissions scenario tropical storms are more likely to form closer to the U.S. East Coast and thus closer to the location of this study, Norfolk, VA (Garner et al., 2021). Other studies suggest potential northward expansion in tropical storms and hurricanes due to climate change (Studholme et al., 2022). High-resolution storm surge models show that even small changes in hurricane tracks or timing can result in unpredictable remote impact on the coast and more challenging storm surge predictions (Park et al., 2022).

Recent studies found that in additional to storm surges, hurricanes and tropical storms can have indirect impact on ocean circulation and the coasts. For example, hurricanes like Matthew (2016) and Dorian (2019), which passed along the GS without making landfall in the continental U.S., nevertheless disrupted the flow of the GS and reduced its transport by as much as 50% (Ezer, 2019, 2020b; Ezer et al., 2017; Todd et al., 2018). Such remote influences from offshore storms can raise coastal sea level days after hurricanes disappeared and are difficult to predict. When adding SLR to unpredictable sea level variations that were ignored in the past, may result in additional unpredictable flooding. For example, weak storms or even seasonal high tides can now cause at least minor tidal floods (the so called "nuisance" floods), as evident in many locations (Ezer, 2020a; Ezer & Atkinson, 2014; Sweet et al., 2014). Based on past local information, NOAA defines nuisance threshold exceedance water levels for each U.S. tide gauge location relative to Mean Higher High Water (MHHW), and these values range from 0.25 m in Wilmington, NC, to 0.68 m in Boston, MA (Sweet et al., 2014). However, location-dependence water levels make it difficult to compare the impact of SLR on different locations, so in some studies (e.g., Ezer & Atkinson, 2014) fixed thresholds are defined so that minor, moderate and major flood levels are defined as 1 ft (∼0.3 m), 2 ft (∼0.6 m), and 3 ft (∼0.9 m) over MHHW, respectively; these levels have been used here as well. The city of Norfolk was chosen here as an example of city at risk to demonstrate past and future flooding and test new methodologies. In Norfolk for example, many streets start flooding when water level at the Sewell Point tide gauge station nearby reaches ∼0.3 m over MHHW, well before the official NOAA's "nuisance" level of 0.53 m is reached (many of these floods have been documented in pictures taken by the author; see: http://www.ccpo.odu.edu/~tezer/).

To predict future flooding, four main contributors may be considered: future mean SLR, tides, storm surges, and extreme wind waves. However, while wave setup and swash due to high wind waves may have important impact on many coasts, such as sandy beaches along the Pacific Ocean (Melet et al., 2018; Serafin et al., 2017), waves contribution is negligible in Norfolk and other locations in the Chesapeake Bay (CB) that are not directly exposed to Atlantic Ocean wind waves. In Norfolk for example, flooding is caused primarily by SLR and tides in the Elizabeth River (where the tide gauge is located), so wind waves are small and can be neglected. In locations where waves setup contributes significantly to flooding events, this effect may be captured by the water level measurements, and thus a statistical flood model like the one suggested here will indeed include the combined effect of storm surges, tides, and waves. It is possible however that some tide gauges are located where wave setup is significant but cannot be captured by the tide gauge (e.g., a gauge on a pier some distance away from a sandy beach), and in such cases additional observations or wave models can be used to improve the flood prediction, as discussed later. The main goal of the simple statistical model suggested here is to represent the variability and trends of the water level observations and whatever processes they capture; developing physical models of say tides, waves and SLR are beyond the scope of this study.

Several other factors may also affect future flooding such as variations in the GS, changes in the frequency, intensity and track of hurricanes and tropical storms, and other climatic changes in wind patterns, air pressure, and precipitation. Of all these factors, only future tides are relatively predictable, though due to SLR and anthropogenic coastal changes there are also unpredictable changes in tidal range over the years that are different from place to place (Cheng et al., 2017; Lee et al., 2017). In addition, the 18.6-year lunar nodal cycle can impact SLR and high tide water levels (Baart et al., 2011; Haigh et al., 2011), and some studies suggest that solar activity and lunar precessions can affect interannual variations in extreme sea level (Valle-Levinson & Martin, 2020); all these effects are often not been considered in SLR projections, adding uncertainties.

Predicting future flooding must rely on projections of mean SLR by climate models using different scenarios for future greenhouse gas emissions. A set of SLR projections that is widely used for the U.S. Climate assessment

and flood prediction is the NOAA-2017 projections (Parris et al., 2012; Sweet et al., 2017, 2022). For each location the flood prediction must also include local vertical land movement, local tides and probability statistics of extreme sea level events (Buchanan et al., 2016, 2017; Kopp et al., 2017; Sweet & Park, 2014). The NOAA SLR projections together with extreme value statistics for different flood thresholds are used to characterize the increased frequency of nuisance floods (Sweet & Park, 2014; Sweet et al., 2014) and the probability of future high tide flooding around the U.S. coasts (Sweet et al., 2018, 2022). To predict the geographical extent of flooding one may combine SLR projections with hydrodynamic numerical ocean models, as has been recently done for example, by Alarcon et al. (2022) for the Coral Gables region of southern Florida.

The goal of this study is to test a simple flood prediction method that does not require any tidal or hydrodynamic models or probability functions of extreme events as used by most other flood prediction statistical methods (e.g., Buchanan et al., 2016, 2017). Instead, the method uses only hourly water level data from a tide gauge and random sampling of past water levels to estimate the combination of tides, storm surges and all other unpredictable factors (note however that wind waves are neglected here, as discussed before). A demonstration of the method for one city at risk, Norfolk, VA, also found an empirical formula that can provide rough estimates of expected future floods of any level for any future year. Such a result can be helpful for planning for mitigation and adaptation strategies for cities at risk. The suggested method does not intend to replace the more accurate probabilistic-based formal NOAA projections (see latest NOAA report, Sweet et al., 2022), but to provide a simpler alternative as a research and practical tool for rough estimates of future flooding.

The study is organized as follows. First, the data sources are described in Section 2, then results are presented in Section 3, first for past sea level and flooding and then for projection of future floods, finally a summery and conclusions are offered in Section 4.

2. Data Sources

The hourly water level record for Norfolk (at Sewell Point, VA) since 1927 is available from NOAA (https://tidesandcurrents.noaa.gov/waterlevels.html?id=8638610). This station is located at the southern part of the CB (Figure 1) where local SLR is high due to land subsidence (Bekaert et al., 2017; Boon et al., 2010; Eggleston & Pope, 2013; Ezer & Corlett, 2012). For example, in the upper CB SLR is 3.22 mm/y in Baltimore and 3.71 mm/y in Annapolis, while in the lower CB SLR is 4.9 mm/y in Gloucester and 4.73 mm/y in Norfolk (see Figure 1 for locations). Note that these mean SLR rates are linear trends over the entire records, while due to sea level acceleration in the Bay (Ezer & Corlett, 2012) current rates are even higher and close to 6 mm/y after 2000 (Ezer, 2013).

To estimate future flooding, one needs to know the future SLR, which can be obtained from sea level projections based on climate models and different scenarios of greenhouse gas emissions. The mean sea level projections used here (Figure 2a) were obtained from the US Army Corps of Engineers SLR calculator (https://cwbi-app.sec.usace.army.mil/rccslc/slcc_calc.html), using the NOAA-2017 scenarios (Parris et al., 2012; Sweet et al., 2017) and local land subsidence of ~2.5 mm/y in Norfolk. Local SLR rates increase with time for the high-end projections (Figure 2b), so for example, in the intermediate (II) projection SLR increases from ~10 mm/y in 2020 to ~20 mm/y in 2100, while in the most extreme projection SLR may reach over 60 mm/y by 2100. For the calculations performed here, only 3 projections are used: Intermediate-Low (IL), II, and Intermediate-High (IH), which seem as the most likely scenarios (for details of the probability of different SLR projections and the contributions from different components of the climate system, see studies such as Kopp et al. (2017)).

To estimate future floods, one also needs to define exceedance flood levels, noting that different definitions of flood levels have been used in different publications. For example, based on past data NOAA defined nuisance flood level in Norfolk as 0.53 m above MHHW. However, NOAA's nuisance flood levels are different for each station (Sweet et al., 2014, 2018), so it is difficult to compare between locations. Local experience (including the author's neighborhood) shows that many Norfolk's streets start flooding when water level is around 1 foot (~0.3 m) over MHHW at the nearby Sewell Point tide gauge, so for easier comparisons between different locations Ezer and Atkinson (2014) defined minor, moderate, and major flood levels for all locations at fixed levels of 1 ft (~0.3 m), 2 ft (~0.6 m), and 3 ft (~0.9 m), respectively, which are also used in the current study. The main pattern of accelerated flooding does not significantly change when slightly different definitions of flood levels are used (e.g., Sweet & Park, 2014, vs. Ezer & Atkinson, 2014). One of the goals of this study is to develop a general formula that can allow to estimate future floods at any level a user may choose.
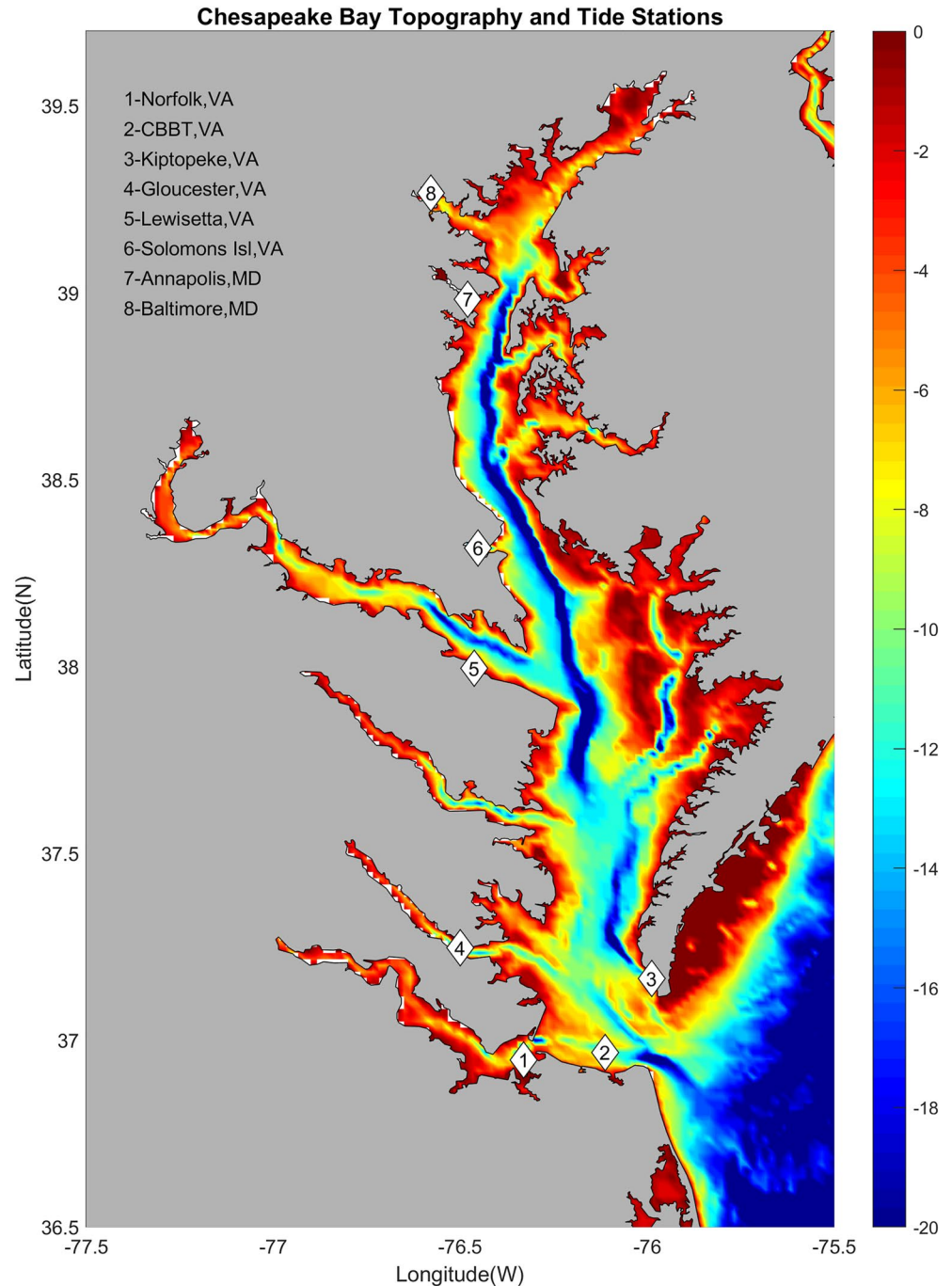
Figure 1. A topographic map (depth in meters) of the Chesapeake Bay and locations of tide gauge stations.

3. Results

3.1. Past Sea Level Rise, Flooding, and Storm Surges

Sea level in Norfolk has been measured almost continuously since 1927, except about a year gap in 1942–1943 and a few smaller gaps (Figure 3a); the measurements are from the NOAA tide gauge at Sewell Point in the southern CB near the intersection of the James River and the Elizabeth River (Figure 1). The largest storm surges in Norfolk, when water level reached at least major flood level of 3 ft (∼0.9 m) over MHHW, are shown in Figure 3b. These storm surges are the result of hurricanes, tropical storms, nor'easters and in some cases winter
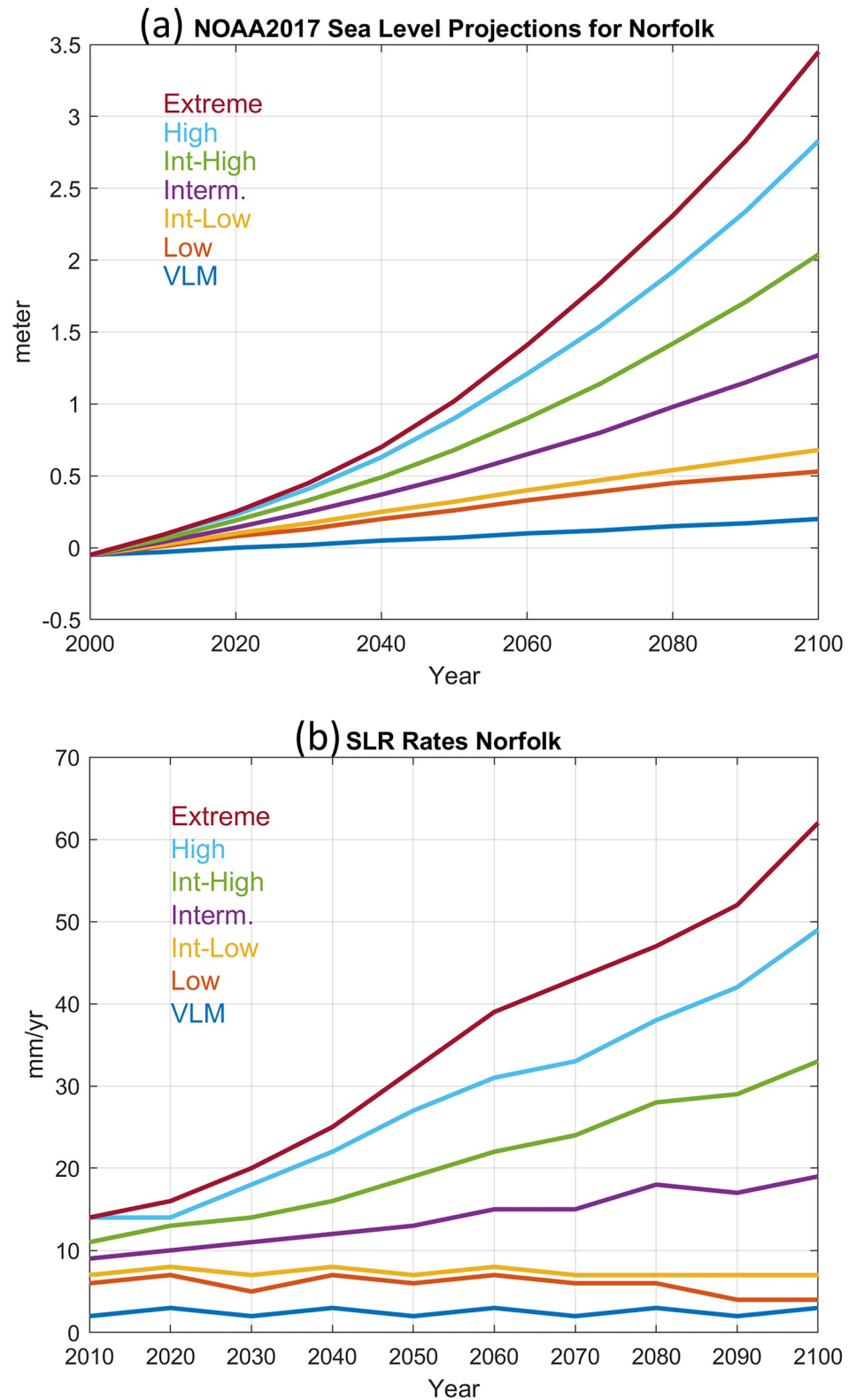
Figure 2. (a) The NOAA2017 sea level projections for Norfolk from lowest to highest: vertical land movement only, low, intermediate-low, intermediate, intermediate-high, high, and extreme projections. (b) Sea level rise (SLR) rates for different projections calculated for each decade (i.e., the SLR in 2100 is calculated from the change from 2090 to 2100).
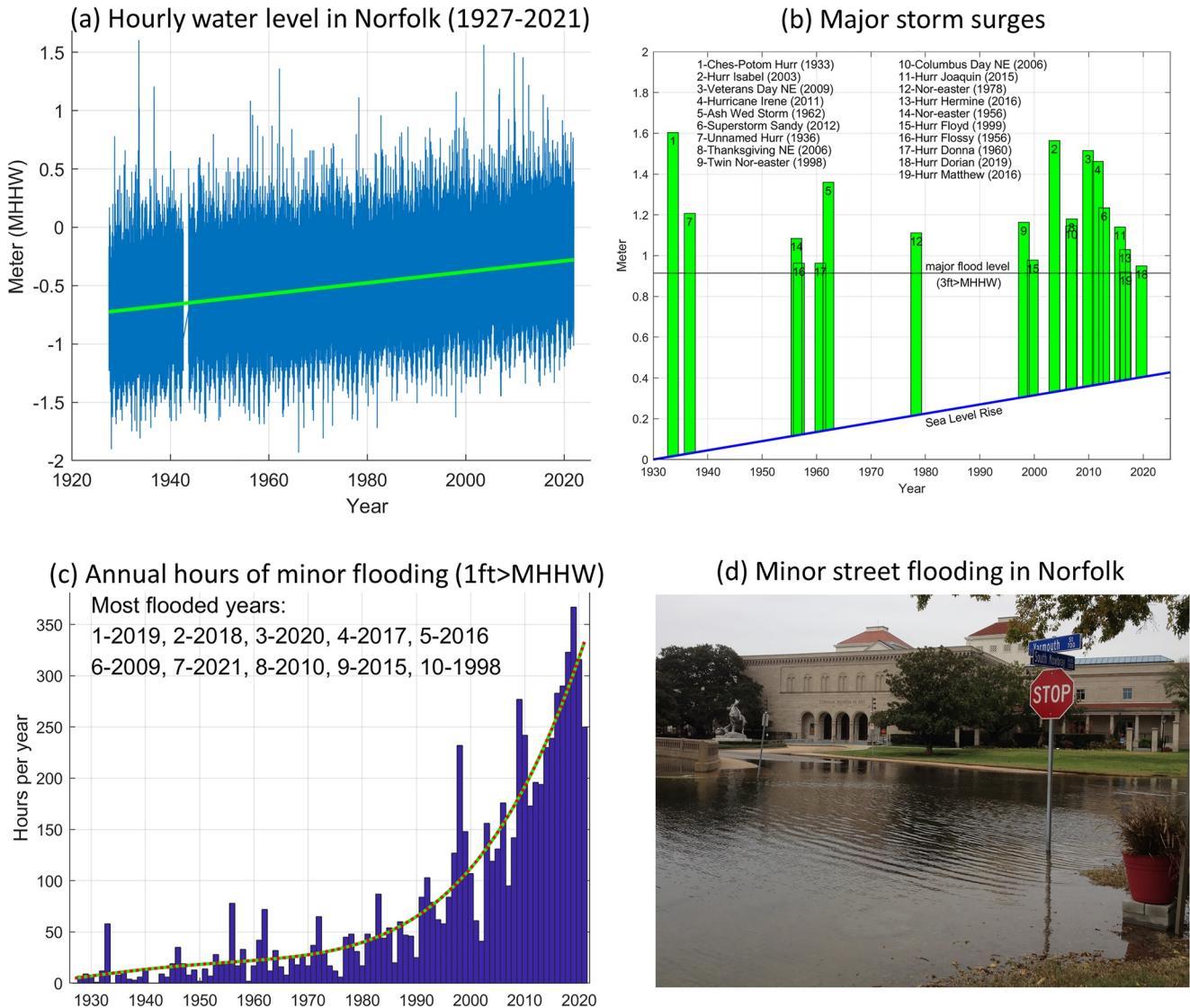
(a) Hourly water level in Norfolk (1927-2021)

(b) Major storm surges

1-Ches-Potom Hurr (1933)   10-Columbus Day NE (2006)
2-Hurr Isabel (2003)   11-Hurr Joaquin (2015)
3-Veterans Day NE (2009)   12-Nor-easter (1978)
4-Hurricane Irene (2011)   13-Hurr Hermine (2016)
5-Ash Wed Storm (1962)   14-Nor-easter (1956)
6-Superstorm Sandy (2012)   15-Hurr Floyd (1999)
7-Unnamed Hurr (1936)   16-Hurr Flossy (1956)
8-Thanksgiving NE (2006)   17-Hurr Donna (1960)
9-Twin Nor-easter (1998)   18-Hurr Dorian (2019)
                              19-Hurr Matthew (2016)

(c) Annual hours of minor flooding (1ft>MHHW)

Most flooded years:
1-2019, 2-2018, 3-2020, 4-2017, 5-2016
6-2009, 7-2021, 8-2010, 9-2015, 10-1998

(d) Minor street flooding in Norfolk

Figure 3. (a) Hourly water level in Norfolk, VA (Sewell Point tide gauge station) and linear trend (zero line is Mean Higher High Water, MHHW). (b) Top storm surges that reached major flood level of at least 3 ft (~0.9 m) over MHHW. (c) Number of hours per year of minor flooding when water level is greater than 1 ft (~0.3 m) above MHHW. (d) Example of minor street floods in Norfolk; this picture of the Chrysler Art Museum was taken by the author in 5-November 2017 during the seasonal "King Tide" (no storm) when water level in Sewell Point was about 0.4 m over MHHW.

extra-tropical storms. In several cases, these storm surges involve hurricanes that did not make landfall in the region, but nevertheless caused indirect impacts by disrupting the flow of the GS which elevated coastal sea level during and after the storms disappeared, as seen for example, during Hurricanes Matthew in 2016 (Ezer et al., 2017), Irma, Jose and Maria in 2017 (Todd et al., 2018), and Dorian in 2019 (Ezer, 2020b). Other hurricanes that caused significant flooding (see labels in Figure 3b) without landfall in the area include Sandy (2012), Joaquin (2015), and Hermine (2016). Hurricanes that passed very close to Norfolk and caused direct storm surge include the Chesapeake-Potomac hurricane (1933), Isabel (2003), and Irene (2011). The former group of offshore hurricanes that did not pass near Norfolk caused weaker storm surges, but with elevated water level that lasted longer (days to weeks), while the latter hurricanes that passed near Norfolk caused larger storm surges, but for a shorter period of hours. Therefore, flood prediction models must account for not only the direct impact of storm surges, which are well understood, but also unpredictable remote influences as well (Park et al., 2022).

In the past, a period of up to ~15 years without any major storm surge was not uncommon (Figure 3b), but since ~1998 major storm surges became very common-the likely explanation is that weaker storms that in the past

caused little or no floods, can now reach a higher flood level with the additional SLR. Change in frequency or path of storms can also contribute to this trend. Minor floods that cause disruption to transportation and daily life accelerated significantly in recent years, as seen in the number of annual hours of minor flooding (Figure 3c). In the past, minor floods happened mostly during storm events, but now the increase frequency of these floods is the direct consequence of SLR. Therefore, minor floods that in average flooded streets ~20 hr per year until the 1980s now accounts for ~200–350 annual hours of floods over the past decade, that is, 10-fold increase. Figure 3d shows a typical minor flood in the Ghent historic district of Norfolk when street floods almost reached the steps of the well-known Chrysler Museum of Art in the background. This type of flood event is often known as a "sunny day flood" without any storm; in this case (November 2017) the flood occurred during the so-called fall "King Tide" period when seasonal tides are higher than normal (Ezer, 2020a). These annual King Tide events are now used as citizen science experiments when hundreds of volunteers collect data to help map street floods, calibrate inundation models and sample floodwater for water quality analysis (Hutton & Allen, 2021; Loftis et al., 2019; Macias-Tapia et al., 2021).

3.2. Future Projections of Floods

To calculate the probability of future floods, one needs to combine the impact of SLR, tides and storm surges. This is done by extension of past hourly water level (Figure 3a) into the future using SLR projection (Figure 2a), so that future flood hours can be estimated (as in Figure 3c). Timing and amplitude of storm surges are unpredictable and linked with the tidal cycle, so that if a peak of a storm surge coincides with high tide it would result in a larger surge than during a low tide. Therefore, tide-surge interactions are important and sometimes includes also nonlinear interactions; the water level measurements should include the results of these processes. Since it is impossible to predict the timing of future storms with respect to the tidal cycle, it is assumed that the statistics of future storms will generally be like that of past storms when removing SLR effects. With over 800,000 hourly water level measurements during the ~95-year record, it can be assumed that there is enough different combinations of storm surges and tidal cycles, so that random sampling will represent the statistics quite well; there is no attempt here to predict any climate-related changes in the statistics of storms. While the approach taking here used a random sampling of past data, it is acknowledged that more sophisticated methods of the statistical distribution of extreme water level are used by others (e.g., Sweet et al., 2022). Note that water level anomaly refers here to anomaly relative to SLR trend which includes tides. A different approach would remove tides to obtain subtidal water level anomaly, however, then tide prediction will be needed for future flood prediction. This approach would not change the main results, but would require a tidal model, and the goal here is to have as simple a method as possible without usage of additional models. The method includes the following steps:

Step-1: Detrend the past water level data 1927–2021 by removing linear trend and calculate hourly anomaly. These water level anomalies ΔSL (t) for 1927–2021 represent the combined tides, storm surges and other unpredictable factors like variations in the GS or air pressure. Although there is some sea level acceleration, at first order a linear trend is quite good estimate as seen in Figure 3a.

Step-2: Choose SLR projections-most likely scenarios would be the three NOAA projections IL, II, and IH. Then find polynomial fits to these projections that will represent mean SLR for 2000–2100,

$$\text{MSL}_p(t) = A_p + B_p t + C_p t^2 \qquad (1)$$

where A, B, and C are the regression coefficients for the 3 projections (subscript "p").

Step-3: Combine the mean sea level projection with a random sampling of past sea level anomaly,

$$\text{SL}(t) = \text{SL}(2021) + \text{MSL}_p(t) + \text{RAND}[\Delta SL(t)] \qquad (2)$$

where SL (2021) adjusts the NOAA projections for 2000–2100 to start at level close to the last year of the past observations in 2021. The results of these projections are shown in Figure 4. Viewing how hourly sea level could look like in the future seems like a useful way to demonstrate to flood-prone locations the potential impact, compared with showing exceedance probability distribution which may not be well understood by the general public when trying to interpret how their street would be affected. Note that the tidal range in Norfolk experienced a small decrease over time, potentially due to SLR (Cheng et al., 2017; Lee et al., 2017). While it is not clear if this trend will continue and by how much, a slight adjustment was made to the amplitude of the last term in Equation 2
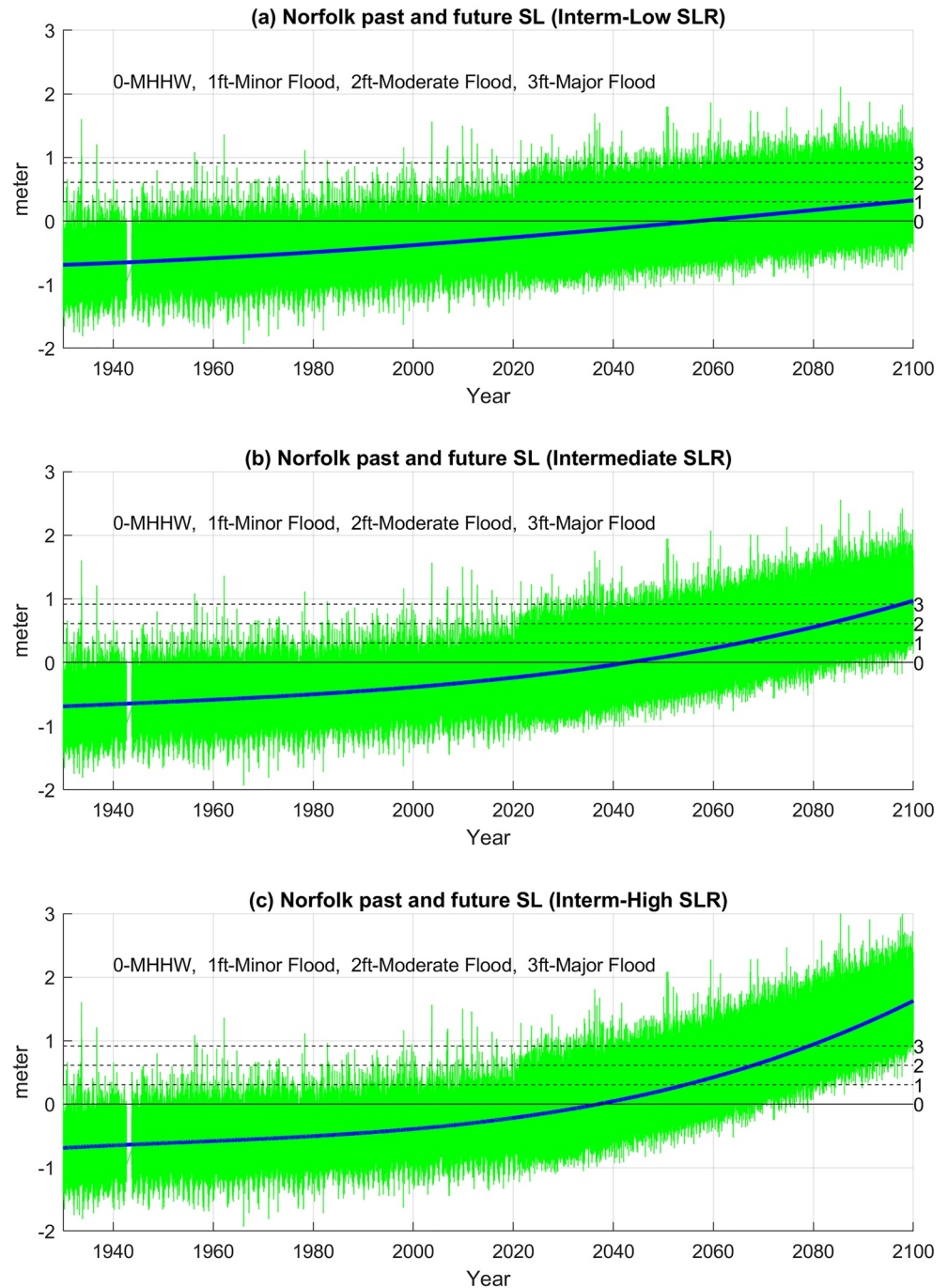
Figure 4. The observed (1927–2021) and projected (2022–2100) hourly water level for 3 sea level projections, (a) intermediate-low, (b) intermediate and (c) intermediate-high. Polynomial fit of mean sea level is marked by heavy blue lines and horizontal black lines represent different water levels.

so that variability at the beginning of the projection is close to that of the last decade in the observations. While there are clear uncertainties in the future tides and storm surges, and impacts from the 18.6-year nodal cycle (Baart et al., 2011; Haigh et al., 2011), or wind waves (Melet et al., 2018) are neglected here, SLR seems to dominate the future sea level compared with other factors. Even for the lower projection (IL), the water level of the highest tides with no surge (MHHW is level zero in Figure 4) will become the water level during low tide by 2100. And for II and IH projections, minor floods (1 ft; ~0.3 m) and major floods (3 ft; ~0.9 m), respectively, will become the norm even during low tides. Compared with the maximum storm surges in the past (Figure 3b) that
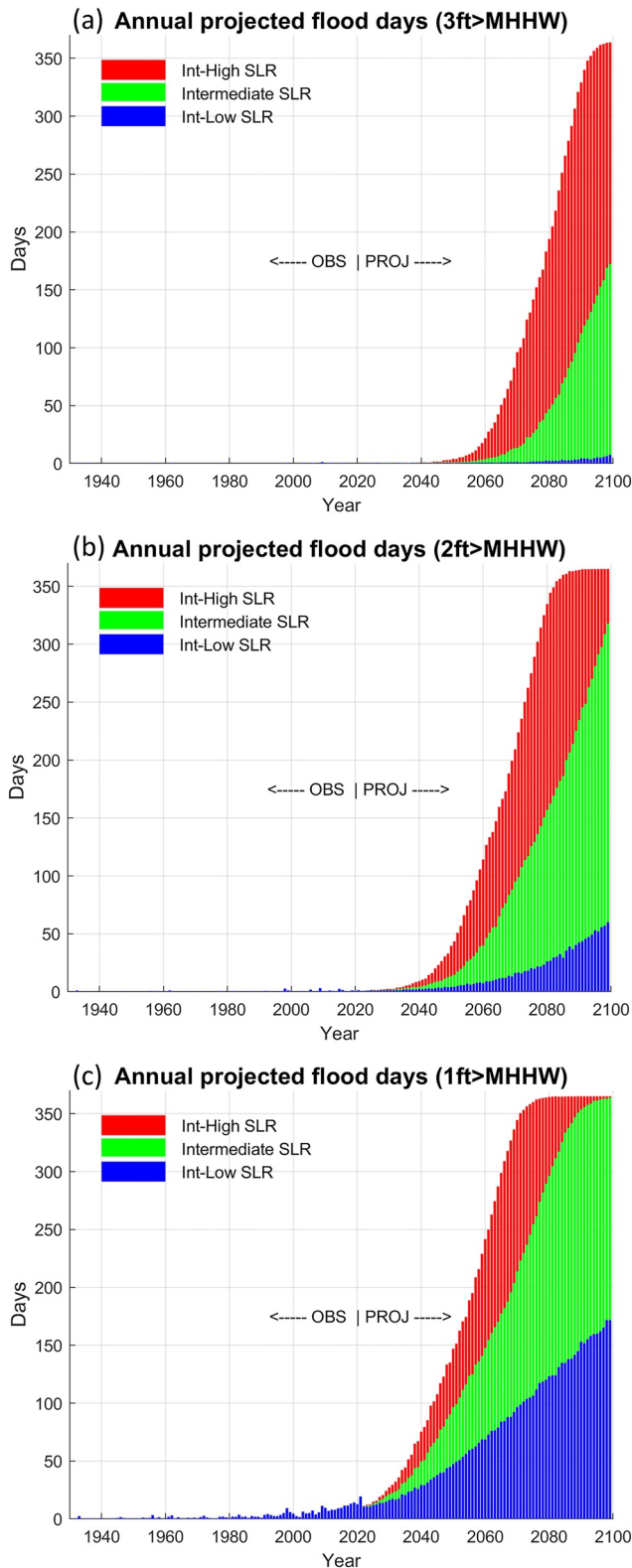
Figure 5. Past and projected annual days of flooding of (a) 1 ft, (b) 2 ft and (c) 3 ft. Blue bars represent past data and intermediate-low sea level projection, green and red bars represent intermediate and intermediate-high projections, respectively.

reached 1.5 m over MHHW only 3 times in 90 years, maximum future surges may reach ~2, 2.5, and 3m, for the 3 projections, IL, II, and IH, respectively.

Step-4: Now, from the hourly sea level for 1927–2100 (Figure 4) it is straight forward to calculate the annual period of flooding (Figure 5) and the probability of flooding (Figure 6) for a given period, flood level and projection. Unlike other studies (e.g., Buchanan et al., 2016) no assumption about the shape of the exceedance probability function is assumed, though it is simply the results of the hourly data for 1927–2100, allowing to compare past and future flood probabilities.

Figure 5 shows the number of days of flooding for the 3 SLR projections (blue, green, and red colors for IL, II, and IH, respectively) and for the 3 levels of flooding (5a, 5b, and 5c). The results here are consistent with NOAA's projections of probability of floods (Sweet et al., 2018), though the method they used is somewhat more complicated, as explained before; here, the only data needed is past water level observations. Comparing the different SLR projections, there is much higher uncertainty in predicting major floods (Figure 5a) with almost 2 orders of magnitude difference between flood time of low and high projections, while for minor floods the difference is much smaller, ~50%. For the high SLR projection, continuous flooding (every hour, 365 days a year) will occur for minor flooding around 2070, for moderate flooding around 2090 and for major flooding by 2100. Even under low SLR projections, minor floods will occur about half of the time by 2100 (blue in Figure 5c), which is enough to cause major disruption to many city roads. An example of the probability of past and future sea level and associated flooding probability are shown in Figure 6 for the II projections. From 1940s to 2020 minor floods (blue vertical lines) became more common while major floods were still quite rare (upper 4 panels of Figure 6; see also Figure 3). However, the probability of floods increases significantly in the future (lower 4 panels of Figure 6), so that by 2060–2080 minor floods become the most common, occurring about half of the time and by 2080–2100 moderate floods become the most common.

So far, only the distribution of future water level from random sampling of past data is shown (Figure 6), but this analysis cannot account for the potential impact in the future from very infrequent storm surges (say "50 to 100-year storms," such as the two largest hurricane storm surges of 1933 and 2003, Figure 3b). Therefore, additional calculations are made with 1000 simulations, each realization has different random sampling of the ~800,000 hourly past water level anomalies on top of the II SLR scenario. From the ensemble of these simulations the probability of annual maximum water level was calculated and shown in Figure 7 for 2050 and 2100. Unlike other studies that assume a particular shape of probability for extreme value distribution (e.g., Sweet et al., 2022), here the results are the distribution of the data itself. The result of the probability distribution is clearly non-Gaussian with a long tail for extreme high values (~20-year storms and higher; right side of the distribution). Therefore, rare big storms may cause extreme water level of over 2 m (above MHHW) in 2050 and almost 3 m in 2100. In the year 2100 there is over 60% chance of extreme water level reaching between 2.1 and 2.4 m. In comparison, during the last two decades (2000–2020) the mean annual maximum water level was less than 1 m. For higher SLR projections, even more dramatic increase in extreme water level is expected, so the distribution in Figure 7 can be easily adjusted (shifted to the right) for any future SLR.

Returning to the example of random sampling in Figures 4–6, the probability of floods for all 3 projections and 3 flood levels is summarized in Figure 8a,
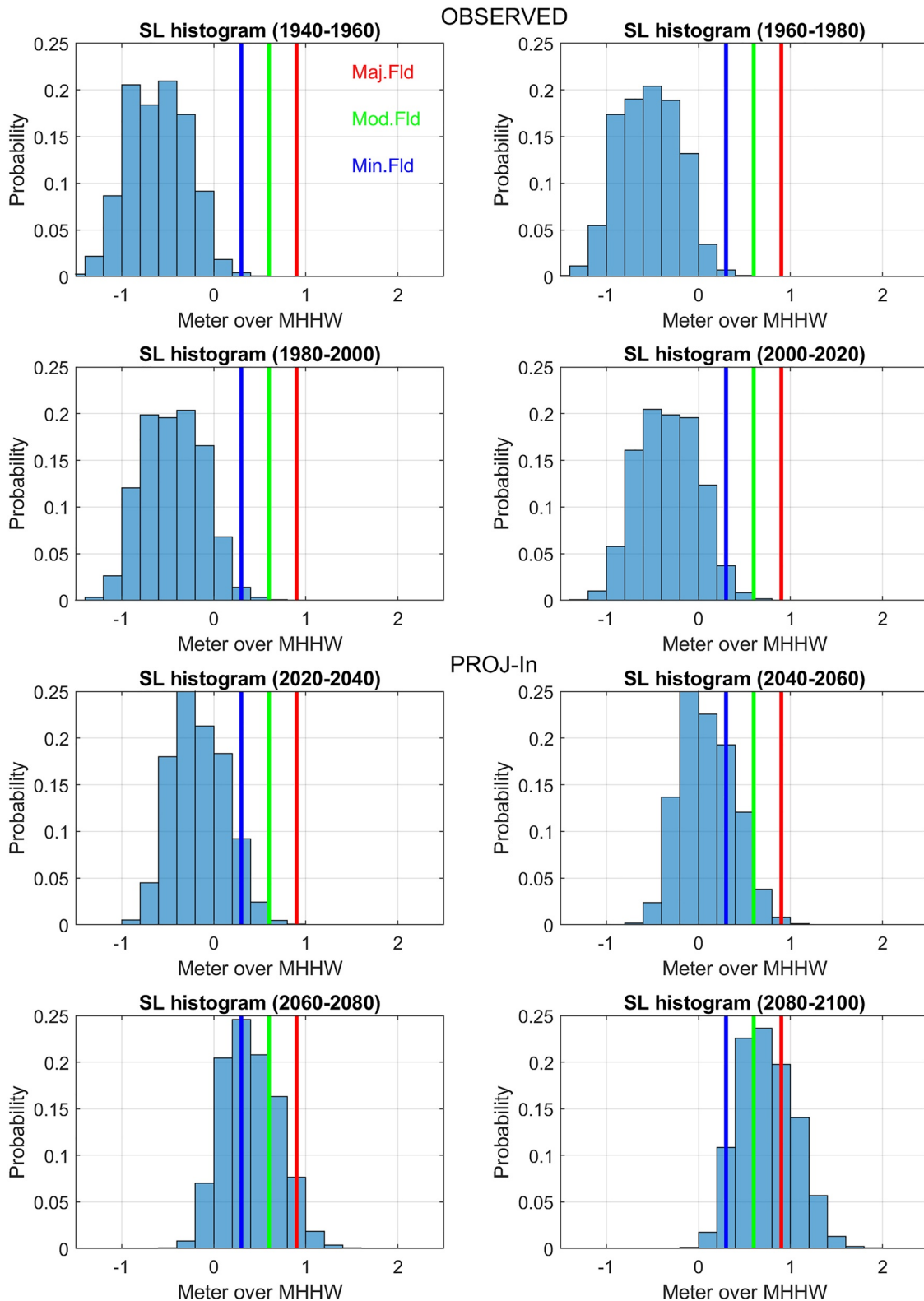
Figure 6. Probability distribution of water level for each 20-year period: top 4 panels are from observed past data and bottom 4 panels are from the intermediate sea level projection. Vertical bars represent minor flood level (1 ft, blue), moderate flood level (2 ft, green) and major flood level (3 ft, red).
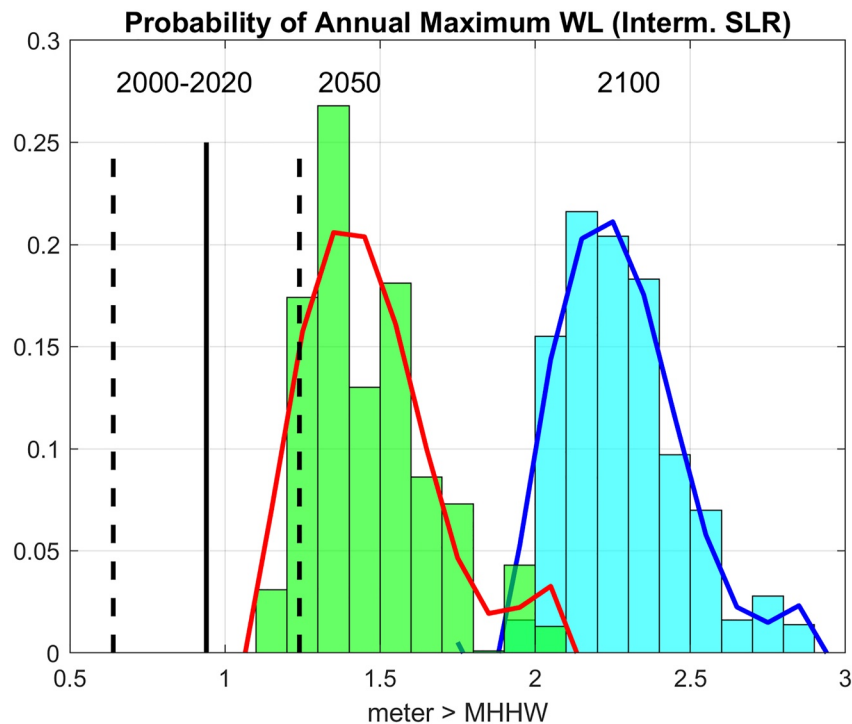
Figure 7. Probability of annual maximum water level for 2050 (green bars; red line is polynomial fit) and for 2100 (cyan bars; blue line is polynomial fit), calculated from 1000 simulations of randomly sampling past water level anomaly on top of the intermediate sea level rise scenario. For comparison, the mean and standard deviation of maximum water level during the period 2000–2020 is also shown (vertical black lines).

showing the percentage of flood time in the hourly record for every 20-year period from 1940 to 1960 until 2080–2100 (note the logarithmic scale). As indicated before, for minor flooding the difference between the different projections is relatively smaller than for major floods; the latter depends on rare events with poor past statistics while the former is linked directly with SLR. From the percentage of flood time, return period (sometimes called "exceedance probability") is calculated. For example, moderate floods in the 1960s occurred ~0.02% of the time, that is $0.02 \times 365 \times 24/100 = 1.75$ hr of floods per year meaning that water level exceeds 2 ft more than once a year (return period <1 year); by the 2020s such floods will occur over ~0.2% of the time (~1.5 hr per month; return period <1 month), and by 2100 under low SLR projection such floods will occur over ~10% of the time (~2.4 hr per day; return period ~10 hr, meaning about every peak of the semidiurnal tide). Note however that the hourly return period calculated here is different than the Average Recurrence Interval (ARI) if calculated on daily basis. For example, a storm surge with water level over 1m that occurs on average once a year would have ARI = 1, but if each storm causes say 4 hr of flooding, the hourly based return period would be 3 months. Since the method presented here does not rely on probability function of exceedance events as other methods do, it is constructive to evaluate if it is consistent with other methods. For example, interpolating the results of Sweet and Park (2014) for the probability of exceedance in Norfolk (their Figure 9) into percent of flooding time for minor flood (1 ft > MHHW), they obtained in 2010 ~3% flood time at that level compared with ~2.5% here. And comparing the projected probability of NOAA's nuisance flooding exceedance in Norfolk (0.53 m > MHHW) for 2010–2100 (Figure 10 in Sweet & Park, 2014) with Figure 8a shows that their NCA-Low projection gives similar results to the IL projection here, and their RCP-8.5 projection gives results similar to the IH projection here; both methods indicate that projections of flooding in 2100 has very large differences between the different scenarios (much larger range of possibilities than the difference between methods).

One interesting result from Figure 8 is that the past increase in flooding (black lines) and the IL projection of future flooding (blue lines) are closely sitting on the same linear line on a logarithmic scale. This means that the same logarithmic acceleration in flooding applied to past and future floods for this projection (except when reaching close to the limit of 100%). This projection can be assumed as an estimate for minimum potential future flooding, and in this case an empirical flood prediction estimate is obtained by logarithmic line fitting,
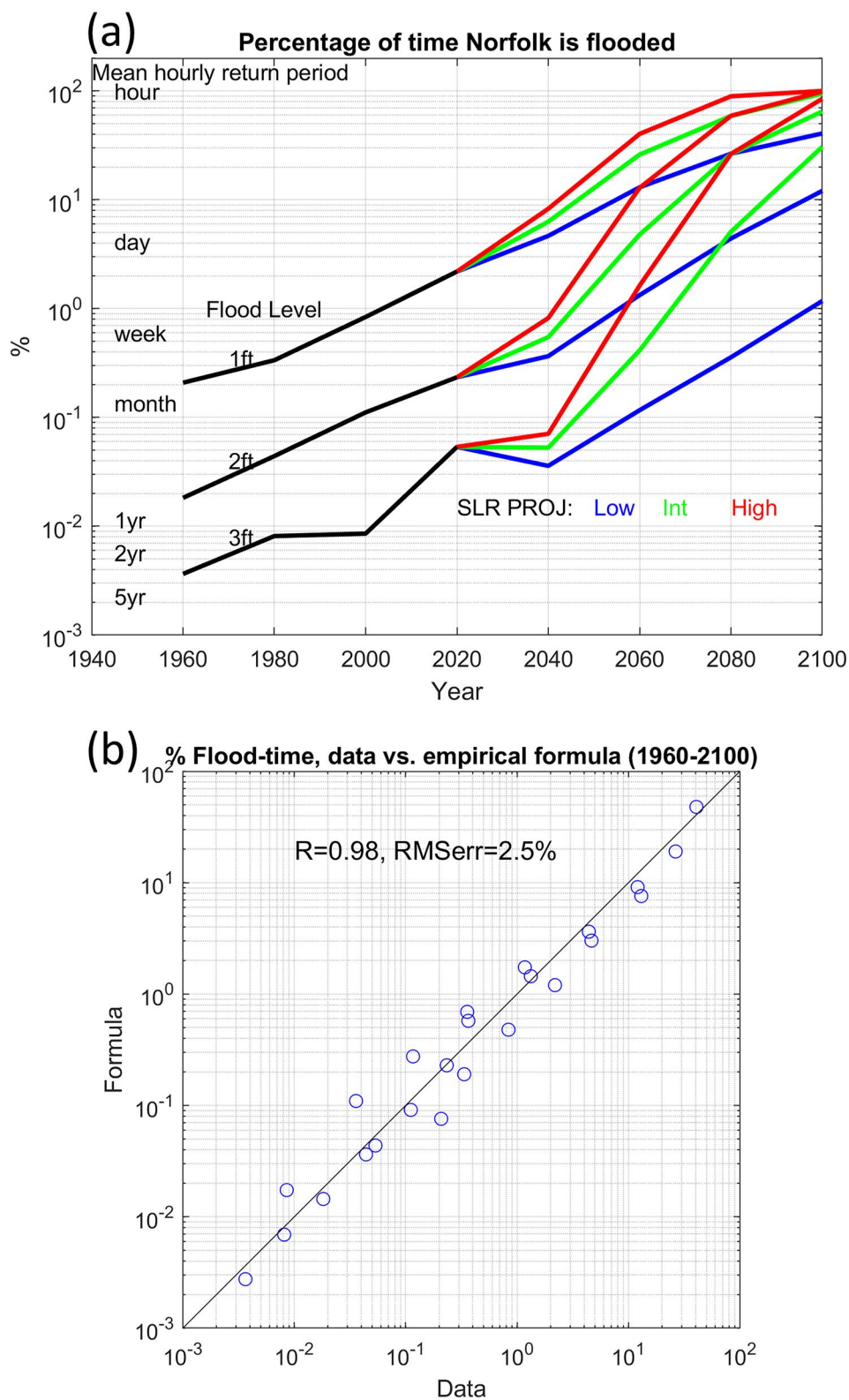
Figure 8. (a) Percent of hourly flood time for 3 different flood levels for past data (black lines) and 3 sea level projections (color lines); values are shown at the end of each 20-year period (1940–1960 to 2080–2100). Estimated return period of hourly flood is also indicated. (b) A comparison of the percentage flooding time between the data in Figure 8a (past data and intermediate-low projection; black and blue lines) and estimation from Equation 3; Correlation coefficient (R) and root-mean-square error are indicated.
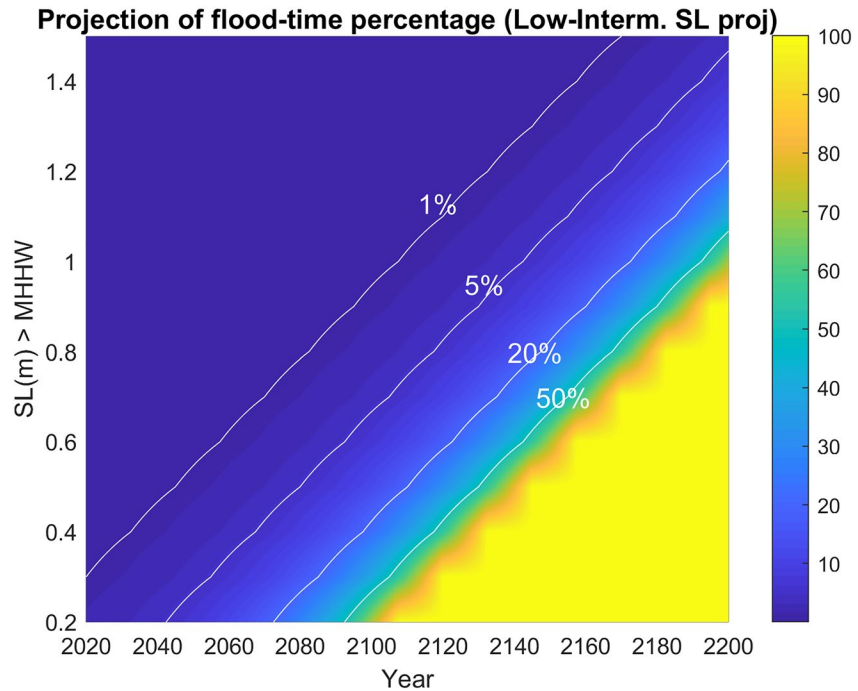
Projection of flood-time percentage (Low-Interm. SL proj)

Figure 9. Probability of floods (in percentage of time) for different flood levels (*y*-axis in meters above mean higher high water) for intermediate-low sea level projection; figure is based on Equation 3.

$$P(\%) = 10^A; A(Y, F) = 0.02Y - 2.4F - 39.6 \tag{3}$$

where P is the percentage of time that hourly flood at level F (meter > MHHW) occurs in year Y. Figure 8b compares Equation 3 with the data in Figure 8a, showing high correlation ($R = 0.98$) and relatively small mean error (RMSerr = 2.5%). This empirical projection of Equation 3 is depicted in Figure 9. From Equation 3 one can easily estimate the year in which flood occurs every hour (i.e., $P = 100\%$) under IL SLR projection,

$$Y(100\%) = 2080 + 120F \tag{4}$$

From Equation 4 one can infer that water level of today's high tide (MHHW, $F = 0$) will occur 100% of the time sometimes before 2080 (since Equation 4 is for low projection). In comparison, in the past 60 years MHHW level increased from occurring ∼0.3% of the time in the 1960s to ∼6% in 2021, but it will reach 100% in the next 60 years under IL projection of SLR (and much sooner for other projections). Minor and major floods of $F = 0.3$ and 0.9 m will occur all the time at a minimum around the years 2116 and 2188, respectively. However, without mitigations such as relocation or raising houses, low-laying locations will became unhabitable years before floods occur all the time, since even floods that occur 1% of the time means flooding more than once a week, which likely disrupts daily life and transportation on major roads.

4. Summary and Discussion

Since sea level is expected to rise for decades to come, the frequency and severity of floods will continue to accelerate, especially along the U.S. coasts where local SLR is higher than global SLR (Ezer & Atkinson, 2014; Kruel, 2016; Sweet & Park, 2014; Sweet et al., 2014, 2017, 2018, 2022; Wdowinski et al., 2016). Due to SLR, damage from storm surges and tidal flooding had increased in the past and will continue to increase in the coming decades (Buchanan et al., 2017; Cazenave & Le Cozannet, 2014; Nicholls & Cazenave, 2010; Taherkhani et al., 2020). Minor (so-called "nuisance") floods already became much more than nuisance in many low-lying coastal communities, affecting transportation, businesses, real estate values, and having a significant economic cost (Hino et al., 2019). The focus of this study was on Norfolk, VA, as an example of a coastal city that is vulnerable to the impact of SLR. However, the methodology presented here can easily apply to many other cities under similar risks, and the simplicity of the method means that only hourly water level data is needed to make

estimated future flood projections. The main approach here assumes that tide gauge measurements can capture the combination of all the factors that impact flooding, such as SLR, tides, storm surges and waves, and the goal is to represent the statistics of the observed water level. However, it should be acknowledged that some processes, such as waves setup on sandy beaches (Melet et al., 2018; Serafin et al., 2017) may not be captured by some tide gauges due to their location, and in these cases additional surf zone wave models or empirical relations between offshore wave measurements and waves setup on the shore may be used to improve the flood prediction.

This study area (including the Hampton Roads region surrounding Norfolk) was chosen as demonstration because the increase in flooding at this region already led to various initiatives to address public awareness and plan mitigation and adaptation strategies. These activities include for example, citizen science projects of monitoring street flooding and associated water quality issues (Hutton & Allen, 2021; Macias-Tapia et al., 2021), engagement with local stakeholders (John & Yusuf, 2019; Yusuf et al., 2018) and development of sensor network and flood prediction systems (Loftis et al., 2019).

Planning for potential future flooding cannot rely solely on sea level projection (which are obtained from climate models under different greenhouse gas emissions), because in addition to local SLR, flood prediction needs to consider also tides, storm surges and extreme wind waves. Several unpredictable factors can further affect coastal sea level such as short-term (Ezer, 2016) and long-term (Ezer, 2015; Ezer et al., 2013) variations in the GS; changes in hurricane tracks or intensity (Ezer, 2019; Garner et al., 2021; Park et al., 2022; Studholme et al., 2022) or variations in the El-Nino Southern Oscillations, ENSO (Sweet et al., 2018), the AMOC (Ezer & Dangendorf, 2020), and the North Atlantic Oscillations, NAO (Ezer & Dangendorf, 2022). NOAA provides flood prediction reports for the U.S. coasts (Sweet et al., 2014, 2017, 2018, 2022) that are based on statistical probabilistic approach to account for the expected frequency of storm surge events. These projections, together with land topography and numerical models can be used to predict the extent of inundations (Alarcon et al., 2022; Loftis et al., 2019). Note however that the statistics of storm surge may change from place to place and over time. The approach taken here is somewhat simpler, since it does not require any models or prior knowledge of the probability of storm events, and instead rely solely on publicly available hourly water level data. The idea is to randomly sample observed detrended sea level anomalies to represent the combined impacts of tides, storm surges and all other unpredictable factors. For the Norfolk's tide gauge, the result is an hourly water level record from 1927 to 2100, which allows to directly view and compare the probability of past floods (1927–2021) with future floods (1921–2100). The calculations were done for 3 flood levels and 3 SLR projections. Future minor floods (1 ft or ∼0.3 m > MHHW) are determined almost completely by SLR, and by 2100 they will occur almost 100% of the time for the II SLR projection and ∼50% of the time for IL projection (which is enough to make some low-level streets impossible for usage). However, major floods (3 ft or ∼0.9 m > MHHW) are less predictable, so the percentage of time that streets are flooded at that level by 2100 range between 1% for IL SLR projection to almost 100% for IH SLR projection. The probability of maximum annual storm surge was calculated using ensemble of 1000 simulations, showing that even for II SLR scenario, maximum water level may reach over 2 m above the high tide in 2050 and near 3 m by 2100. In comparison, over the past ∼90 years water level reached 1.5 m only 3 times (during major hurricanes). This calculation demonstrates the importance of considering not only the most likely scenarios, but also the low probability extreme rare storm events. An interesting result of the study is that on a logarithmic scale the increase in flood probability of the past and the IL projections are in line, allowing to empirically estimate minimum level of flooding for any year 1960–2100 and for any flood level.

In summary, the study describes the observed impacts of SLR on flooding in the city of Norfolk as an example to demonstrate a simple method to predict the probability of future floods. The results show that past acceleration in flooding is likely to continue as sea level continues to rise. A simple empirical prediction formula was found that can be used as a practical tool for providing rough estimates of lower limit of future flooding in particular location. It is noted that this formula for Norfolk is not intended to replace the official NOAA flood prediction for the entire U.S. coast, but to provide an additional tool for researchers and stakeholders. Better understanding of the factors affecting future flooding can help planning for mitigation and adaptation strategies for many other cities under risk due to SLR.

Data Availability Statement

The hourly tide gauge sea level record for Norfolk is available from NOAA (https://tidesandcurrents.noaa.gov/waterlevels.html?id=8638610), and the sea level rise projections are available from USACE (https://cwbi-app.sec.usace.army.mil/rccslc/slcc_calc.html). Analysis and graphic tools are based on standard Matlab codes (https://www.mathworks.com/products/matlab.html).

References

Alarcon, V. J., Linhoss, A. C., Kelble, C. R., Mickle, P. F., Sanchez-Banda, G. F., Mardonez-Meza, F. E., et al. (2022). Coastal inundation under concurrent mean and extreme sea-level rise in Coral Gables, Florida, USA. *Natural Hazards*, *111*(3), 2933–2962. https://doi.org/10.1007/s11069-021-05163-0

Baart, F., van Gelder, P. H., de Ronde, J., van Koningsveld, M., & Wouters, B. (2011). The effect of the 18.6-year lunar nodal cycle on regional sea-level rise estimates. *Journal of Coastal Research*, *28*(2), 511–516. https://doi.org/10.2112/JCOASTRES-D-11-00169.1

Bekaert, D. P. S., Hamlington, B. D., Buzzanga, B., & Jones, C. E. (2017). Spaceborne synthetic aperture radar survey of subsidence in Hampton Roads, Virginia (USA). *Scientific Reports*, *7*(1), 14752. https://doi.org/10.1038/s41598-017-15309-5

Boon, J. D. (2012). Evidence of sea level acceleration at U.S. and Canadian tide stations, Atlantic coast, North America. *Journal of Coastal Research*, *28*(6), 1437–1445. https://doi.org/10.2112/JCOASTRES-D-12-00102.1

Boon, J. D., Brubaker, J. M., & Forrest, D. R. (2010). Chesapeake Bay land subsidence and Sea level change: An evaluation of past and present trends and future outlook. In *Special report in applied marine science and ocean engineering* (Vol. 425). Virginia Institute of Marine Science. https://doi.org/10.21220/V58X4P

Buchanan, M. K., Kopp, R. E., Oppenheimer, M., & Tebaldi, C. (2016). Allowances for evolving coastal flood risk under uncertain local sea-level rise. *Climate Change*, *137*(3–4), 347–362. https://doi.org/10.1007/s10584-016-1664-7

Buchanan, M. K., Oppenheimer, M., & Kopp, R. E. (2017). Amplification of flood frequencies with local sea level rise and emerging flood regimes. *Environmental Research Letters*, *12*(6), 064009. https://doi.org/10.1088/1748-9326/aa6cb3

Buzzanga, B., Bekaert, D. P. S., Hamlington, B., & Sangha, S. S. (2020). Toward sustained monitoring of subsidence at the coast using InSAR and GPS: An application in Hampton Roads, Virginia. *Geophysical Research Letters*, *47*(18). https://doi.org/10.1029/2020GL090013

Cazenave, A., & Le Cozannet, G. (2014). Sea level rise and its coastal impacts. *Earth's Future*, *2*(2), 15–34. https://doi.org/10.1002/2013EF000188

Cheng, Y., Ezer, T., Atkinson, L. P., & Xu, Q. (2017). Analysis of tidal amplitude changes using the EMD method. *Continental Shelf Research*, *148*, 44–52. https://doi.org/10.1016/j.csr.2017.09.009

Domingues, R., Goni, G., Baringer, M., & Volkov, D. (2018). What caused the accelerated sea level changes along the U.S. East Coast during 2010–2015? *Geophysical Research Letters*, *45*(24), 13367–13376. https://doi.org/10.1029/2018GL081183

Eggleston, J., & Pope, J. (2013). Land subsidence and relative sea-level rise in the southern Chesapeake Bay region. *US Geological Survey Circular*, *1392*. https://doi.org/10.3133/cir1392

Emanuel, K. (2011). Global warming effects on U.S. hurricane damage. *Weather, Climate, and Society*, *3*(4), 261–268. https://doi.org/10.1175/WCAS-D-11-00007.1

Ezer, T. (2013). Sea level rise, spatially uneven and temporally unsteady: Why the U.S. East Coast, the global tide gauge record and the global altimeter data show different trends. *Geophysical Research Letters*, *40*(20), 5439–5444. https://doi.org/10.1002/2013GL057952

Ezer, T. (2015). Detecting changes in the transport of the gulf stream and the Atlantic overturning circulation from coastal sea level data: The extreme decline in 2009-2010 and estimated variations for 1935-2012. *Global and Planetary Change*, *129*, 23–36. https://doi.org/10.1016/j.gloplacha.2015.03.002

Ezer, T. (2016). Can the gulf stream induce coherent short-term fluctuations in Sea level along the U.S. East Coast? A modeling study. *Ocean Dynamics*, *66*(2), 207–220. https://doi.org/10.1007/s10236-016-0928-0

Ezer, T. (2019). Numerical modeling of the impact of hurricanes on ocean dynamics: Sensitivity of the gulf stream response to storm's track. *Ocean Dynamics*, *69*(9), 1053–1066. https://doi.org/10.1007/s10236-019-01289-9

Ezer, T. (2020a). Analysis of the changing patterns of seasonal flooding along the U.S. East Coast. *Ocean Dynamics*, *70*(2), 241–255. https://doi.org/10.1007/s10236-019-01326-7

Ezer, T. (2020b). The long-term and far-reaching impact of hurricane Dorian (2019) on the gulf stream and the coast. *Journal of Marine Systems*, *208*, 103370. https://doi.org/10.1016/j.jmarsys.2020.103370

Ezer, T., & Atkinson, L. P. (2014). Accelerated flooding along the U.S. East Coast: On the impact of sea-level rise, tides, storms, the gulf stream, and the North Atlantic oscillations. *Earth's Future*, *2*(8), 362–382. https://doi.org/10.1002/2014EF000252

Ezer, T., Atkinson, L. P., Corlett, W. B., & Blanco, J. L. (2013). Gulf stream's induced sea level rise and variability along the U.S. mid-Atlantic coast. *Journal of Geophysical Research*, *118*(2), 685–697. https://doi.org/10.1002/jgrc.20091

Ezer, T., Atkinson, L. P., & Tuleya, R. (2017). Observations and operational model simulations reveal the impact of Hurricane Matthew (2016) on the gulf stream and coastal sea level. *Dynamics of Atmospheres and Oceans*, *80*, 124–138. https://doi.org/10.1016/j.dynatmoce.2017.10.006

Ezer, T., & Corlett, W. B. (2012). Is sea level rise accelerating in the Chesapeake Bay? A demonstration of a novel new approach for analyzing sea level data. *Geophysical Research Letters*, *39*(19). https://doi.org/10.1029/2012GL053435

Ezer, T., & Dangendorf, S. (2020). Global sea level reconstruction for 1900-2015 reveals regional variability in ocean dynamics and an unprecedented long weakening in the gulf stream flow since the 1990s. *Ocean Science*, *16*(4), 997–1016. https://doi.org/10.5194/os-16-997-2020

Ezer, T., & Dangendorf, S. (2022). Spatiotemporal variability of the ocean since 1900: Testing a new approach using global sea level reconstruction. *Ocean Dynamics*, *72*(1), 79–97. https://doi.org/10.1007/s10236-021-01494-5

Garner, A. J., Kopp, R. E., & Horton, B. P. (2021). Evolving tropical cyclone tracks in the North Atlantic in a warming climate. *Earth's Future*, *9*(12), e2021EF002326. https://doi.org/10.1029/2021EF002326

Haigh, I. D., Eliot, M., & Pattiaratchi, C. (2011). Global influences of the 18.61 year nodal cycle and 8.85 year cycle of lunar perigee on high tidal levels. *Journal of Geophysical Research*, *116*(C6), C06025. https://doi.org/10.1029/2010JC006645

Hino, M., Belanger, S. T., Field, C. B., Davies, A. R., & Mach, K. J. (2019). High-tide flooding disrupts local economic activity. *Science Advances*, *5*(2). https://doi.org/10.1126/sciadv.aau2736

Hutton, N. S., & Allen, T. R. (2021). Perceptions of visual and in situ representations of sea level rise and tidal flooding: The blue line project, Norfolk, Virginia. *Geojournal*, *87*(3), 2081–2099. https://doi.org/10.1007/s10708-020-10356-4

Jevrejeva, S., Grinsted, A., & Moore, J. C. (2009). Anthropogenic forcing dominates sea level rise since 1850. *Geophysical Research Letters*, *36*(20), L20706. https://doi.org/10.1029/2009GL040216

John, S. B., III, & Yusuf, J. E. (2019). Perspectives of the expert and experienced on challenges to regional adaptation for sea level rise: Implications for multisectoral readiness and boundary spanning. *Coastal Management*, *47*(2), 151–168. https://doi.org/10.1080/08920753.2019.1564951

Knutson, T. R., Camargo, S. J., Chan, J. C. L., Emanuel, K., Ho, C.-H., Kossin, J., et al. (2019). Tropical cyclones and climate change assessment: Part II. Projected response to anthropogenic warming. *Bulletin of the American Meteorological Society*, *101*(3), 303–322. https://doi.org/10.1175/BAMS-D-18-0194.1

Kopp, R. E., DeConto, R. M., Bader, D. A., Hay, C. C., Horton, R. M., Kulp, S., et al. (2017). Evolving understanding of Antarctic ice-sheet physics and ambiguity in probabilistic sea-level projections. *Earth's Future*, *5*(12), 1217–1233. https://doi.org/10.1002/2017EF000663

Kopp, R. E., Horton, R. M., Little, C. M., Mitrovica, J. X., Oppenheimer, M., Rasmussen, D. J., et al. (2014). Probabilistic 21st and 22nd century sea-level projections at a global network of tide-gauge sites. *Earth's Future*, *2*(8), 383–406. https://doi.org/10.1002/2014EF000239

Kruel, S. (2016). The impacts of sea-level rise on tidal flooding in Boston, Massachusetts. *Journal of Coastal Research*, *32*(6), 1302–1309. https://doi.org/10.2112/JCOASTRES-D-15-00100.1

Lee, S. B., Li, M., & Zhang, F. (2017). Impact of sea level rise on tidal range in Chesapeake and Delaware Bays. *Journal of Geophysical Research*, *122*(5), 3917–3938. https://doi.org/10.1002/2016JC012597

Lobeto, H., Menendez, M., & Losada, I. J. (2021). Future behavior of wind wave extremes due to climate change. *Scientific Reports*, *11*(1), 7869. https://doi.org/10.1038/s41598-021-86524-4

Loftis, J. D., Mitchell, M., Schatt, D., Forrest, D. R., Wang, H. V., Mayfield, D., & Stiles, W. A. (2019). Validating an operational flood forecast model using citizen science in Hampton Roads, VA, USA. *Journal of Marine Science and Engineering*, *7*(8), 242. https://doi.org/10.3390/jmse7080242

Macias-Tapia, A., Mulholland, M. R., Selden, C. R., Loftis, J. D., & Bernhardt, P. W. (2021). Effects of tidal flooding on estuarine biogeochemistry: Quantifying flood-driven nitrogen inputs in an urban, lower Chesapeake Bay sub-tributary. *Water Research*, *201*, 117329. https://doi.org/10.1016/j.watres.2021.117329

Melet, A., Meyssignac, B., Almar, R., & Le Cozannet, G. (2018). Under-estimated wave contribution to coastal sea-level rise. *Nature Climate Change*, *8*(3), 234–239. https://doi.org/10.1038/s41558-018-0088-y

Mitchell, M., & Bilkovic, D. M. (2019). Embracing dynamic design for climate-resilient living shorelines. *Journal of Applied Ecology*, *56*(5), 1099–1105. https://doi.org/10.1111/1365-2664.13371

Nicholls, R. J., & Cazenave, A. (2010). Sea-level rise and its impact on coastal zones. *Science*, *328*(5985), 1517–1520. https://doi.org/10.1126/science.1185782

Park, J., & Sweet, W. (2015). Accelerated sea level rise and Florida current transport. *Ocean Science*, *11*(4), 607–615. https://doi.org/10.5194/os-11-607-2015

Park, K., Federico, I., Di Lorenzo, E., Ezer, T., Cobb, K. M., Pinardi, N., & Coppini, G. (2022). The contribution of hurricane remote ocean forcing to storm surge along the Southeastern U.S. coast. *Coastal Engineering*, *173*, 104098. https://doi.org/10.1016/j.coastaleng.2022.104098

Parris, A., Bromirski, P., Burkett, V., Cayan, D., Culver, M., Hall, J., et al. (2012). Global sea level rise scenarios for the US national climate assessment. *NOAA Tech Memo OAR CPO-1*. (Vol. *37*). Retrieved from: https://scenarios.globalchange.gov/sites/default/files/NOAA_SLR_r3_0.pdf

Sallenger, A. H., Doran, K. S., & Howd, P. A. (2012). Hotspot of accelerated sea-level rise on the Atlantic coast of North America. *Nature Climate Change*, *2*(12), 884–888. https://doi.org/10.1038/nclimate1597

Serafin, K. A., Ruggiero, P., & Stockdon, H. F. (2017). The relative contribution of waves, tides, and nontidal residuals to extreme total water levels on U.S. West Coast sandy beaches. *Geophysical Research Letters*, *44*(4), 1839–1847. https://doi.org/10.1002/2016GL071020

Studholme, J., Fedorov, A. V., Gulev, S. K., Emanuel, K., & Hodges, K. (2022). Poleward expansion of tropical cyclone latitudes in warming climates. *Nature Geoscience*, *15*(1), 14–28. https://doi.org/10.1038/s41561-021-00859-1

Sweet, W., Dusek, G., Obeysekera, J., & Marra, J. J. (2018). *Patterns and projections of high tide flooding along the U.S. coastline using a common impact threshold* (p. 44). NOAA Technical report NOS CO-OPS 086, NOAA, Silver Spring, MD. Retrieved from https://tidesandcurrents.noaa.gov/publications/techrpt86_PaP_of_HTFlooding.pdf

Sweet, W., Hamlington, B. D., Kopp, R. E., Weaver, C. P., Barnard, P. L., Bekaert, D., et al. (2022). Global and regional sea level rise scenarios for the United States: Updated mean projections and extreme water level probabilities along U.S. coastlines. In *NOAA technical report NOS 01* (p. 111). National Oceanic and Atmospheric Administration, National Ocean Service, Silver Spring, MD. Retrieved from https://oceanservice.noaa.gov/hazards/sealevelrise/noaa-nos-techrpt01-global-regional-SLR-scenarios-US.pdf

Sweet, W., Kopp, R. E., Weaver, C. P., Obeysekera, J., Horton, R. M., Thieler, E. R., & Zervas, C. (2017). *Global and regional sea level rise scenarios for the United States* (p. 64). NOAA Technical report NOS CO-OPS 083, NOAA Silver Spring, MD. Retrieved from https://tidesandcurrents.noaa.gov/publications/techrpt83_Global_and_Regional_SLR_Scenarios_for_the_US_final.pdf

Sweet, W., & Park, J. (2014). From the extreme to the mean: Acceleration and tipping points of coastal inundation from sea level rise. *Earth's Future*, *2*(12), 579–600. https://doi.org/10.1002/2014EF000272

Sweet, W., Park, J., Marra, J., Zervas, C., & Gill, S. (2014). *Sea level rise and nuisance flood frequency changes around the United States* (p. 58). NOAA Technical report NOS CO-OPS 073, NOAA Silver Spring, MD. Retrieved from https://repository.library.noaa.gov/view/noaa/30823

Taherkhani, M., Vitousek, S., Barnard, P. L., Frazer, N., Anderson, T. R., & Fletcher, C. H. (2020). Sea-level rise exponentially increases coastal flood frequency. *Scientific Reports*, *10*(1), 6466. https://doi.org/10.1038/s41598-020-62188-4

Todd, R. E., Asher, T. G., Heiderich, J., Bane, J. M., & Luettich, R. A. (2018). Transient response of the gulf stream to multiple hurricanes in 2017. *Geophysical Research Letters*, *45*(19). https://doi.org/10.1029/2018GL079180

Valle-Levinson, A., Dutton, A., & Martin, J. B. (2017). Spatial and temporal variability of sea level rise hot spots over the eastern United States. *Geophysical Research Letters*, *44*(15), 7876–7882. https://doi.org/10.1002/2017GL073926

Valle-Levinson, A., & Martin, J. B. (2020). Solar activity and lunar precessions influence extreme sea-level variability in the U.S. Atlantic and Gulf of Mexico coasts. *Geophysical Research Letters*, *47*(20), e2020GL090024. https://doi.org/10.1029/2020GL090024

Wdowinski, S., Bray, R., Kirtman, B. P., & Wu, Z. (2016). Increasing flooding hazard in coastal communities due to rising sea level: Case study of Miami Beach, Florida. *Ocean & Coastal Management*, *126*, 1–8. https://doi.org/10.1016/j.ocecoaman.2016.03.002

Yusuf, J. E., John, B. S., III, Covi, M., & Nicula, J. G. (2018). Engaging stakeholders in planning for sea level rise and resilience. *Journal of Contemporary Water Research & Education*, *164*(1), 112–123. https://doi.org/10.1111/j.1936-704X.2018.03287.x